Research article

Detailed tectonic geomorphology of the Dras fault zone, NW Himalaya

AA Shah[1],*, A Rajasekharan[1], N Batmanathan[2], Zainul Farhan[1], Qibah Reduan[1] and JN Malik[3]

[1] Department of Geosciences, Universiti Brunei Darussalam, Brunei
[2] Southeast Asia Disaster Prevention Research Initiative, Universiti Kebangsaan Malaysia
[3] Department of Earth Sciences, Indian Institute of Technology Kanpur, India

* Correspondence: Email: afroz.shah@ubd.edu.bn; Tel: +6738370102.

Abstract: Our recent mapping of the Dras fault zone in the NW Himalaya has answered one of the most anticipated searches in recent times where strike-slip faulting was expected from the geodetic studies. Therefore, the discovery of the fault is a leap towards the understanding of the causes of active faulting in the region, and how the plate tectonic convergence between India and Eurasia is compensated in the interior portions of the Himalayan collision zone, and what does that imply about the overall convergence budget and the associated earthquake hazards. The present work is an extended version of our previous studies on the mapping of the Dras fault zone, and we show details that were either not available or briefly touched. We have used the 30 m shuttle radar topography to map the tectonic geomorphological features that includes the fault scarps, deflected drainage, triangular facets, ridge crests, faulted Quaternary landforms and so on. The results show that oblique strike-slip faulting is active in the suture zone, which suggests that the active crustal deformation is actively compensated in the interior portions of the orogen, and it is not just restricted to the frontal portions. The Dras fault is a major fault that we have interpreted either as a south dipping oblique backthrust or an oblique north dipping normal fault. The fieldwork was conducted in Leh, but it did not reveal any evidence for active faulting, and the fieldwork in the Dras region was not possible because of the politically sensitive nature of border regions where fieldwork is always an uphill task.

Keywords: active faults; Leh; Dras fault; Kashmir; NW Himalaya

1. Introduction

Tectonic convergence between the lithospheric plates has created several mountain systems in the world, which involved processes such as subduction, magmatism, and collision [1–8]. The crustal

deformation and the structural evolution of the interacting tectonic plates have occurred during the orogenesis, and such imprints are usually preserved in geology, sediments, topography etc. Tectonic geomorphology is a special tool to extract such critical information to map and understand past events [8–13] and to infer future mountain-building processes that involve growth and developments of faults and so on. Although, the Himalayan fault systems are perhaps some of the best-studied faults in the world [14,15], however, the discovery of active unknown faults is an ongoing mission to understand the details of active orogenic processes that have remained largely unexplored and often challenging. The present work further elucidates why tectonic geomorphological studies are needed to understand the active deformation during orogenesis and particularly to map and understand the young orogenic belts such as the Himalayas (Figure 1).

The Himalayan orogenic belt was created by the interaction between the continental plates of India and Eurasia and the active deformation is primarily absorbed in the frontal portions where the Main Frontal Thrust (MHT), a megathrust fault, absorbs ~ half of the plate convergence. Therefore, it is not surprising to discover that many major earthquake events have been largely restricted to the megathrust fault system. However, what is truly surprising is the lack of good quality geological and structural maps, and particularly, in the hinterland region, which has hindered our progress to understand the cause of faulting in the interior portions of the Himalayan orogen. Therefore, our motivation is to improve the mapping of active faults in the NW Himalayan regions, which will provide data to produce reliable structural and seismic hazard maps. The interior faults are expected to accommodate some portion of the regional plate convergence, which makes it imperative to map the hinterland regions with a motivation to understand the causes of active faults and their implication on regional and tectonic scales. We have used tectonic geomorphology as the main tool to investigate and map the evidence of unknown active faults in the NW Himalaya.

Our recent tectonic geomorphological investigation in the hinterland regions of the NW Himalaya has revealed that the ongoing plate convergence is actively compensated by the formation of a large-scale oblique fault. The fault was expected from the previously published geodetic data, and therefore, our work is the first confirmation about the existence of a large-scale active fault zone that we have named as the Dras fault. The work presented here is the extension of our previous work with details on the tectonic geomorphology of the fault zone that were not explored previously. The evidence of active tectonic features was systematically examined by mapping the fault zone using the 30 m shuttle radar topography. The drainage network was superimposed on the satellite images and then mapping was carried out to trace active faults, deflected streams, faulted ridges, shutter ridges, faulted basins, and so on. The tectonic geomorphology was supplemented with earthquake centroid moment tensor (CMT) focal mechanism and seismicity data. The geodetic data are related to the newly identified fault to understand the kinematics of faulting, and to evaluate the potential earthquakes on the fault. The fieldwork in the Leh basin has been done to map the evidence of faulting.

2. Geological and tectonic setting

Geologically, an orogen is composed of complex lithological units and tectonic structures, which generally preserve evidence of geological and tectonic developments in chronological order [16–20]. The Himalayan orogenic system is a perfect example to observe the accretion of microcontinents, flysch complexes, and island arcs, against the southern boundary of Eurasia since the early Paleozoic [21,22].

The study area is represented by the Ladakh Batholith, which is part of the Kohistan-Ladakh arc complex that represents the Island arc system related to the subduction of India under Eurasia, and subsequent deformation plus erosion that eventually exposed the plutons on the surface (Figure 1). The Indus Basin sedimentary record records the subduction, and post-subduction history [23], which suggests accumulation in a forearc basin during the subduction phase, and intermontane sedimentation during the collision and post-collision phases [24,25]. The Quaternary sedimentation in the basin is dominated by the fluvial sedimentation with evidence of past lake-related deposits within the mountains, some near Leh town, indicating glacial melting. Some past studies [26,27] have suggested that the Indus Group developed by the antecedent history of the Indus River, which may not be true as suggested by the sedimentation and tectonic history of the Indus system. Overall, the geological and structural history of the region is packed between the Himalayan frontal thrust system in the south, and the Indus Suture zone in the north, which is reflected by the range of rock and sediments that outcrop on the map view (Figure 1). The Ladakh Batholith is a competent rock that is usually expected to resist deformation, but we show that it is faulted (this study) and deformed dextrally. The Himalayan rocks that outcrop in the south of the suture zone display a remarkable structural disposition where sudden appearance and disappearance of lithologies is suggestive of faulting (Figure 1). For example, the Lower Proterozoic metamorphic rocks are only outcropping in the NW of the Kashmir basin, which is surrounded by the Kohistan-Ladakh batholith. It clearly indicates reverse faulting, and similarly, the abrupt truncation of Tethys and Kohistan-Ladakh batholith in the Kashmir region indicates faulting.

3. Methodology

The 30 m spatial resolution of the Shutter Radar Topographic Mission derived topography is one of the best satellite images to map the regional scale tectonic features for the study area [28–30]. It is primarily chosen because of the reliability, free availability, and easy to process data in ArcGIS software, which is a competent tool to manage large scale data. The images were examined, and active fault mapping was manually achieved by tracing the topographic breaks, deflected streams, faulted surfaces (such as fans, terraces etc.), geological bedding contacts and so on. The Holocene sedimentary deposits were especially targeted and used to map active faults, and relative age relationships were used to constraint ages. If the fault ruptures or uplifts the Holocene deposits it is considered active. However, such relationships are not always straightforward or correct, and details on them are summarized in [31] and therefore, such complexities in the faulting process will not be repeated here. The traced active features were examined in detail using the Google satellite images, which have captured details of the fault zone, and some of these details are briefly shown in our previous work. The areas that were not covered earlier in detail are mapped here along with the new regions to show large portions of the fault zone.

The major river streams were extracted from the 30 m digital elevation model (DEM), which were derived from the Shutter Radar Topographic Mission (SRTM) dataset and processed in the ArcGIS desktop version of the software. The SRTM data are also processed in the Global Mapper 17 that allows the mapping of topographic ridges, which are used for the geomorphological mapping. The ridges were generated by the Find Ridge Tool, by incorporating information such as minimum elevation, sample size etc. The extracted ridge axes were combined with the hillshade images and the river networks in ArcGIS 10.3.
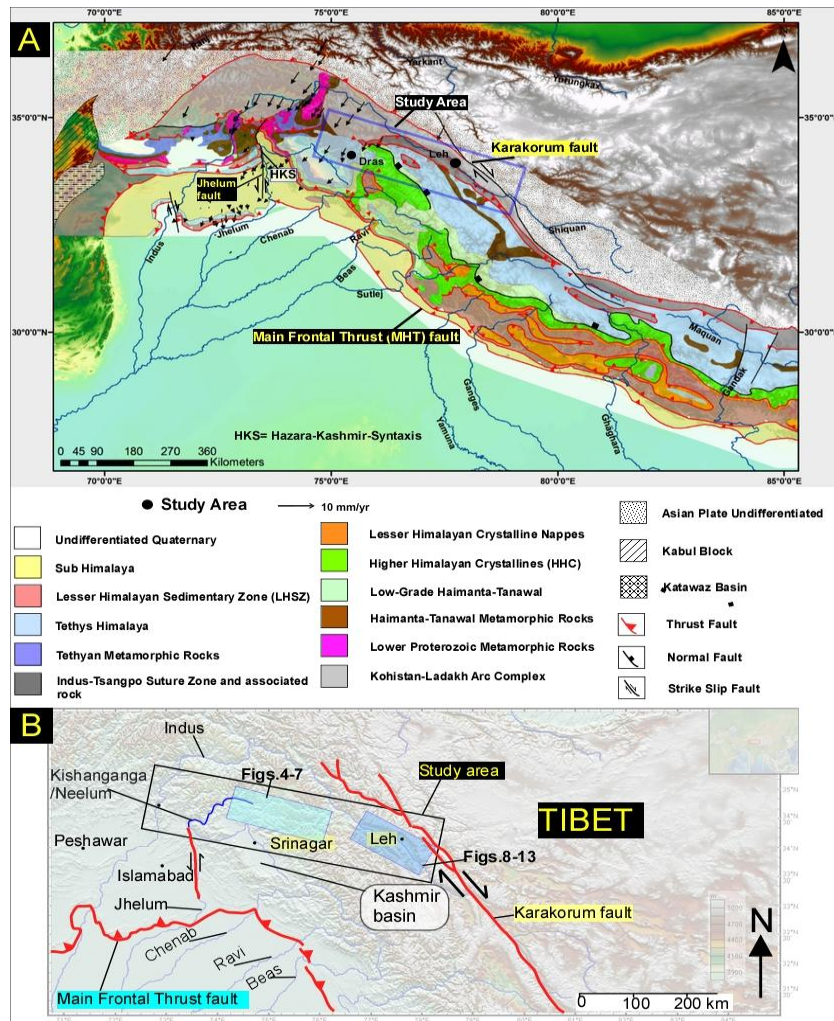
Figure 1. (A) The geological and structural map of [32] is overlaid on the 30m shuttle radar topography to highlight the geological control on topography, and it shows a strong structural control on the geological setting of the NW Himalaya. It is particularly evident in the Hazara-Kashmir-Syntaxis where the Lower Proterozoic Metamorphic rocks are exposed. The geodetic data are also plotted on the map, which is after [33] and suggest oblique convergence in the Kashmir Himalaya. (B) The topographic map shows the three major active faults and rivers in the NW Himalaya and the location of the study area.

Fieldwork was done in the Leh basin to map the evidence for active deformation. The sites were selected based on the geomorphological mapping where the faults were marked prior to visiting the sites. The geological and structural mapping was mainly focused to support the geomorphological observations that we had made based on satellite data interpretations.

We have also used the earthquake centroid moment tensor solutions to map the types of faults, which were correlated with the faults that we had mapped during the geomorphological mapping. The earthquake centroid moment tensor (CMT) data are from the open-source tool, GeoMap App, which covers events from January 1976 to January 2020 (Figure 2). The seismological data have 60 years of spatial coverage (Figure 2) and include events from 1960 until 2020. The geodetic data are after [33] and these data are plotted on the newly identified active faults to understand how the regional plate convergence is accommodated on active faults in the region.

We have also used Seismic Explorer, which uses earthquake data (magnitude, depth, location, time) from the United States Geological Survey. The earthquakes are plotted on the 90m shutter radar topography to show the map view and vertical distribution of shallow crustal events (Figure 3).
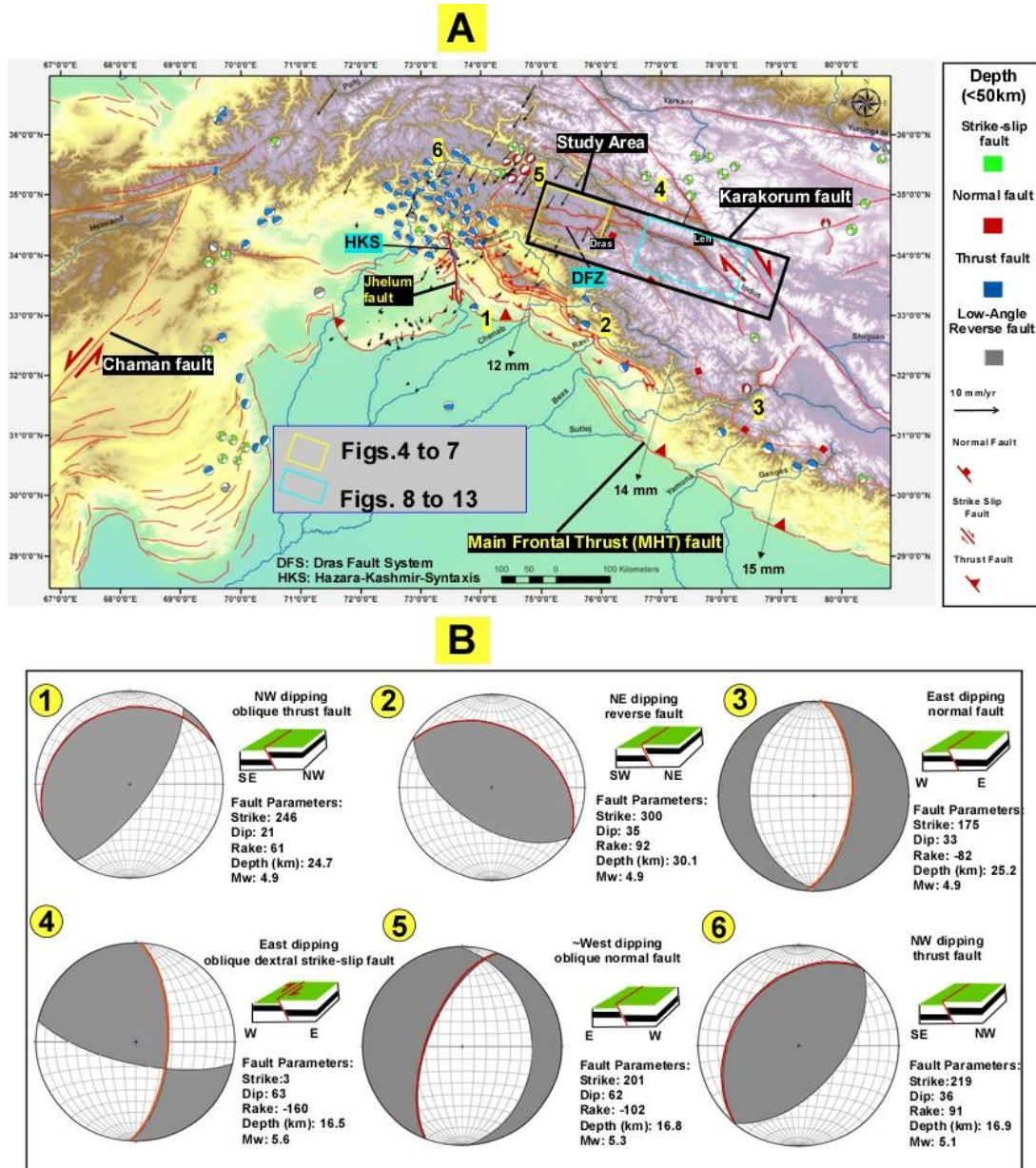

Figure 2. The 30-meter shuttle radar topography is in the background and the earthquake centroid moment tensor (CMT) focal mechanisms are also plotted (coloured beachballs), which mainly suggest ~NW-SE directed shallow crustal extension in the NW portion of the study area. The representative CMT events are numbered, and the details are shown in Figure 2B and explanation in the text.
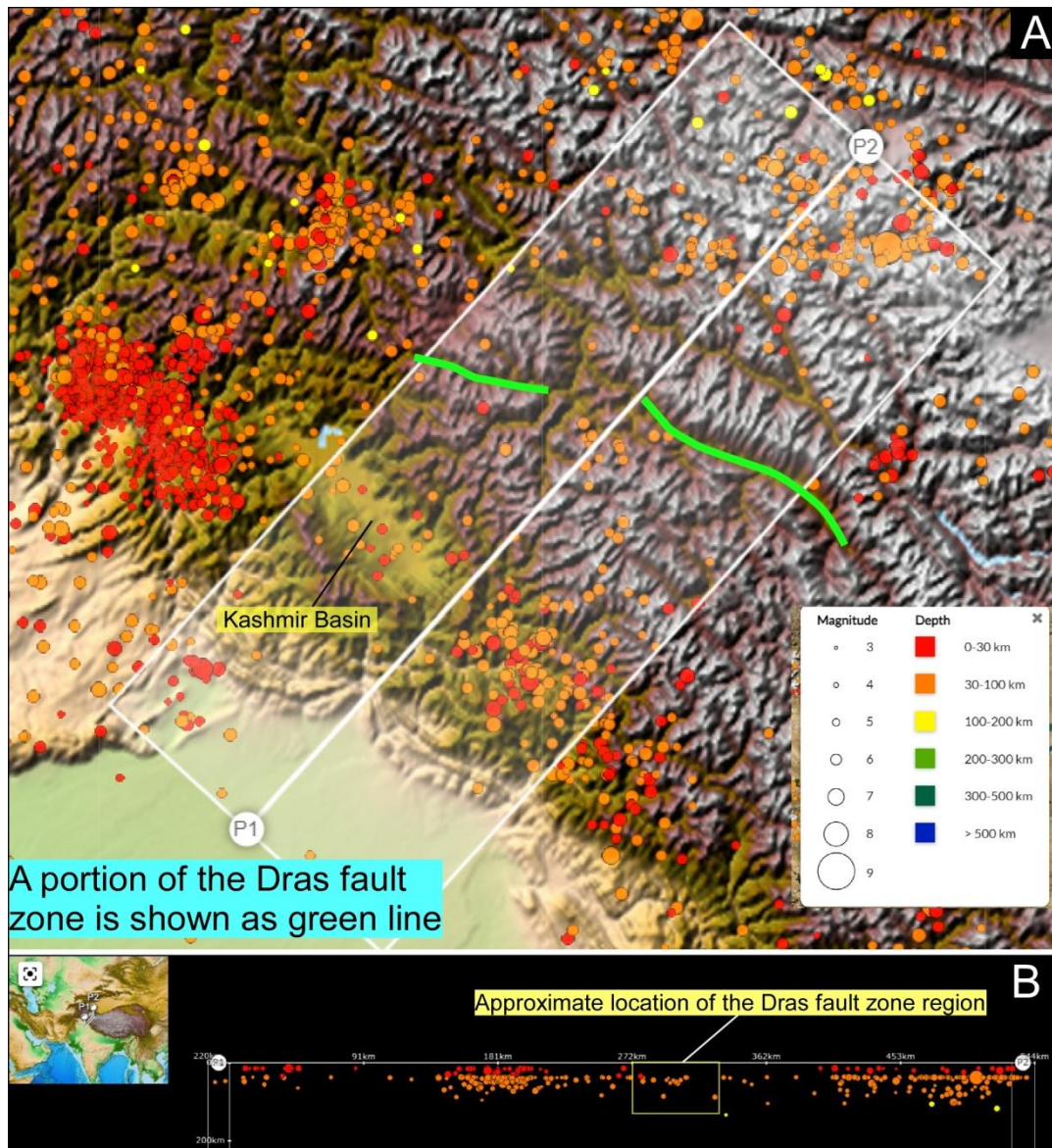
Figure 3. (A) The 90-meter shuttle radar topography is in the background and the earthquake events are plotted (colour filled circles). The two prominent seismicity clusters are at the NW and SE sides of the Kashmir basin. The relatively few events are observed in the north of the Kashmir basin and in the study area. (B) A cross-section is drawn through the study area to show the downdip limit of the observed faulting, which suggest shallow crustal faulting in the region. The figure is made in Seismic Explorer, which uses earthquake data (magnitude, depth, location, time) from the United States Geological Survey.

4. Results and interpretations

4.1. River pattern and active faulting

On a regional scale, the study area is bounded by two major streams: the Kishanganga/Neelum River in the south and the Indus River in the north (Figure 1B). Both these rivers flow towards NNW

before abruptly turning and changing direction towards the southwest. The Kishanganga/Neelum River originates in the Kargil region while the Indus River follows the ~NNW structural trend of the Indus-Tsangpo-Suture zone before turning southwest (Figure 1). These rivers follow the trace of faults, and their orientation is controlled by faults. The left-lateral strike-slip offset of the Jhelum and Indus rivers on the Pakistan side coincides with the active Jhelum and Tarbela fault systems, which are ~N-S trending left-lateral strike-slip faults. The dextral drag on the major streams has caused stream deflections along the trace of the newly mapped Dras fault zone (Figures 4 to 7). These deflections coincide with the similar deflection that we have mapped along the trace of the Dras River (Figure 4). However, such deflections are not observable towards the east of the Dras region, and that includes the Leh basin (Figure 1). Interestingly, a looping pattern of streams was mapped in the Kargil region where an oddly oriented ridge appears and marks the position where rivers loop around (Figures 1 and 4). We have mapped this odd-looking ridge as a restraining bend along the trace of the oblique fault that we have named the Dras fault (see detail below in the proceeding section). The regional geological map shows the trace of the backthrusts that cut across the ridge (Figure 1), but no evidence of such a break could be observed on the satellite image as the ridge is intact (Figures 1 and 4). Instead, we think the ridge is bounded by reverse faults on both sides, which fits a restraining bend structure that could be related to the Dras fault zone.

4.2. Active deformation in the Dras River valley and adjacent regions

We have previously mapped the Dras fault zone [34] and showed the trace of the fault with clear evidence for dextral strike-slip displacement mapped in the Dras region. We further show that the fault zone is wide (Figures 4–6) and extends further east and west. The western extension is marked by two prominent river valleys (Figures 1 and 7) that follow the fault. The Kishanganga River follows the fault, which is suggested by the linear river valley, and the tectonic topography where an elongated ridge is dissected by the fault on both sides. The prominent wineglass canyons and triangular facets are observed on the northern portion (Figure 7) where river streams flow through the canyons and meet the trunk stream, the Kishanganga River (KR). The eastern portion of the KR is faulted, and hence, it is discontinuous. The ~NE-SW trending normal faults have displaced the river, which possibly was continuous in the past (Figure 7). Further west the Neelum River (NR) follows the fault, which is suggested by the faulted ridge crests that would not otherwise be so linearly cut by the river action. The dextral deflection of the major streams also coincides with the strike of the fault, which indicates faulting, and rivers following the trace of the fault. The KG and NR are separated by a ~NE-SW trending fault and we have interpreted the fault as a normal fault, which means that the Dras fault is displaced by the active normal fault (Figure 7). The normal fault-related shallow crustal earthquakes have been reported in the region (Figure 3), and these events support our interpretation. The CMT events shown in Figure 2B are highlighted to show the normal faults and their relationship with the mapped normal faults in the region. The cross-cutting relationships between the normal fault and the Drass fault show that both faults are active, and the normal fault is younger than the Dras fault (Figure 7).

Dras fault is clearly observable in the Dras River valley, which shows dextral strike-slip displacement (Figures 4 to 6). The shutter radar topography shows several displaced and faulted ridges in the valley that can be mapped for >20 km. The Holocene deposits are faulted and the Dras valley is herein interpreted as syntectonic. The ridge in the east is isolated on both sides by the streams, and

since the rocks are competent, therefore, we have interpreted that the rivers are possibly following fault traces that surround the ridge. The ridge fits a restraining bend geometry that would be associated with the oblique Dras fault zone. Figures 5 and 6 show details where dextral strike-slip displacement is clearly observable. The trace of the Dras fault zone is shown in the red line, and the fault is observed to have displaced Holocene sediments, which suggest active faulting. The river terraces, fans, and streams are dextrally offset along the strike of the fault, and the displacement varies from 40 m to > 350 m. Snow has accumulated on the north-facing portion of the fault scarp that has given a unique appearance to the fault trace. Several fans are interpreted to have formed after the faulting (shown in Figure 6), which suggest the age of the latest displacement on the Dras fault: age of sediment accumulation. The tectonic geomorphology reveals that the western portion of the Dras fault zone is mostly represented by rugged topography where the direct evidence of active faulting is not convincing. However, the linearity of major streams suggests faulting. It is also confirmed by the ridge axes that are discontinuous and suggest faulting. The triangular facets are well preserved along some portion of the fault, which also suggests active faulting. The ~NW-SE trending faults are consistent with the strike of the Dras fault zone, which are cut by ~NE-SW trending normal faults.

Overall, the evidence of active faulting in the Dras River valley is convincing, and the curling of the ridge in the east is quite remarkable (Figures 4), and the fault is not observed to pierce through it, which indicates that the fault stops here, and reappears on the eastern portions of the ridge (Figures 8 to 11). The tectonic topography of the region fits a restraining bend geometry, where thrusting would create such a topographical expression of the mapped landforms. Further east, the fault can be traced in the Leh valley (details below).

4.3. Active deformation in Leh and adjacent regions

The entire Leh basin has a striking geomorphic expression on the satellite image of the region (Figures 1 and 2). The geomorphic expression of the basin is equally interesting, and it is broadly divided into two major geomorphic domains: the northwest and southeast of the Phey area (Figure 11). The north-western regions clearly show a broader zone of active deformation where the Himalayan rocks are sandwiched between the two traces of the fault system (Figures 8 to 11). The fault pierces through the Himalayan rocks and juxtaposes them with the Ladakh Batholith that forms the margin of one major fault trace. The faulted and displaced lithological units also contain Quaternary fans and moraines, and the total length of the deformation zone is ~70 km from Phey to Damkhar (Figure 8, upper panel). The total length of the fault zone extends until the Dras region. The fault zone is not mappable in the eastern portions as it is under the blanket of thick sediments in the Leh region that seems to have hidden the evidence for active faulting (Figures 8 and 11). The Indus River follows the trace of the fault and ~borders the Ladakh Batholith from the eastern portions until it reaches the Phey region where it follows another trace of the fault and flows through the Himalayan rocks until the Damkhar area. The vast extent and amazingly looking alluvial fans in the Leh region are cut by the river erosion but the evidence of active faulting was not found in the field (Figure 12). We think the accumulation of the fan-related deposits has forced the river to migrate towards the batholith. However, the fan migration coincides with the bending of the basin and the batholith, which are controlled by faulting (this study). The ~NW-SE trend of the Dras fault zone would be expected to root from the nearby NNW-SSE trending dextral strike-slip fault, the Karakoram fault (Figures 1 and 2), which suggests that the Dras fault zone is the branch of the Karakoram fault system.
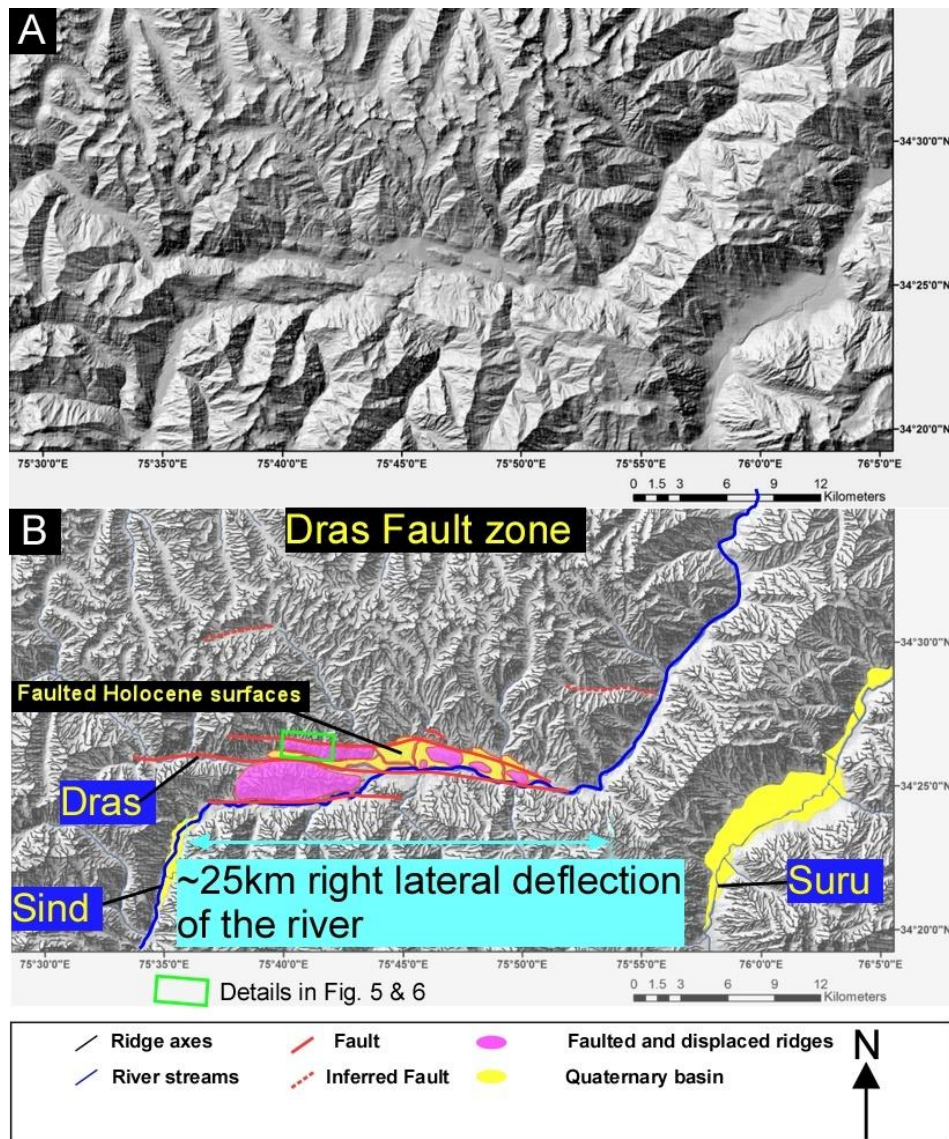
Figure 4. The uninterpreted 30 m shutter radar topographical image (A) is interpreted below (B), and it shows the textbook example of active deformation related to the Dras fault zone. The Holocene deposits are faulted and the Dras valley is herein interpreted as syntectonic. The ridge in the east is isolated on both sides by the streams, and since the rocks are competent, therefore, we have interpreted that the rivers are most possibly following faults. The ridge fits a restraining bend geometry that would be associated with the oblique Dras fault. Figures 5 and 6 show details where dextral strike-slip displacement is clearly observable.
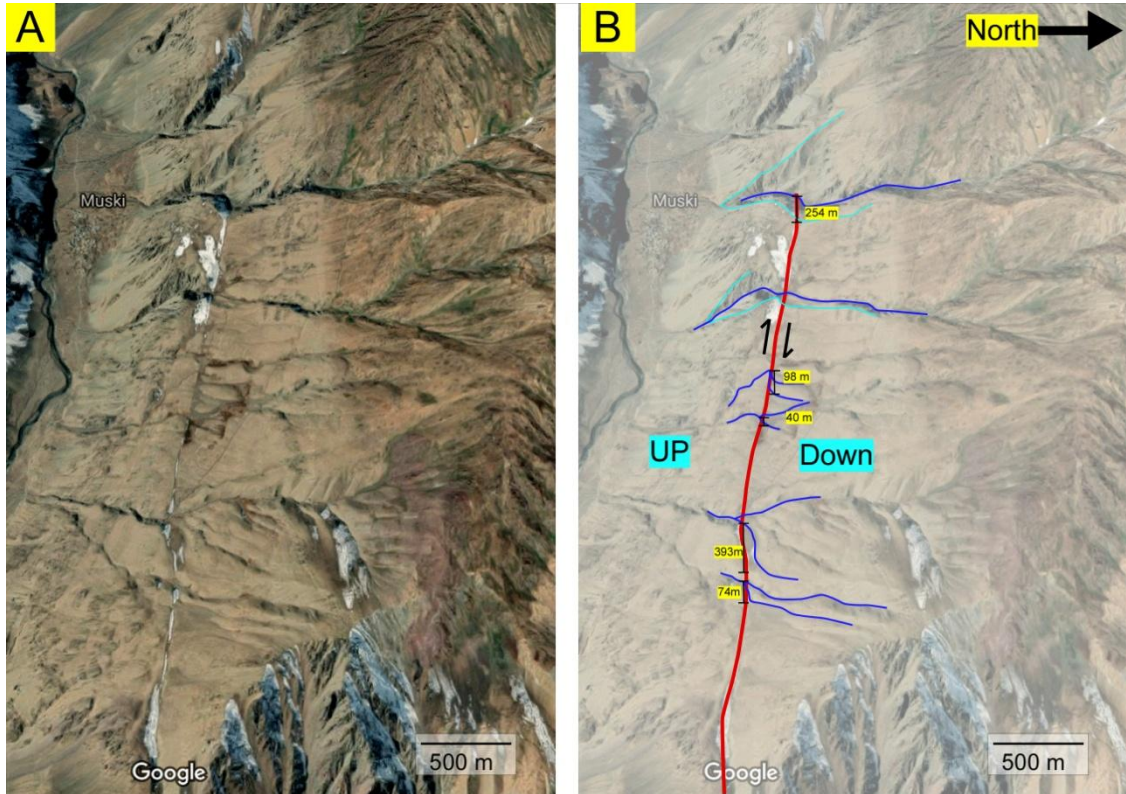
Figure 5. The uninterpreted Google satellite image is shown on left (A) and it is interpreted on right (B). The trace of the Dras fault zone is shown in the red line, which was mapped on the Google satellite image. The fault is observed to have displaced Holocene sediments, which suggest active faulting. The river terraces, fans, and streams are dextrally offset along the strike of the fault, and the displacement varies from 40 m to >350 m. Snow has accumulated on the north-facing portion of the fault scarp that has given a unique appearance to the fault. Several fans have formed after the faulting (shown in Figure 6) and these would suggest the age of faulting, which is the age of sediment accumulation. Therefore, the dating of the fan deposits should directly give the age of faulting. The upthrown (A) and the downthrown blocks are used to interpret the possible dip-slip on the fault, which makes the fault either an oblique normal fault (A) or oblique backthrust (B).
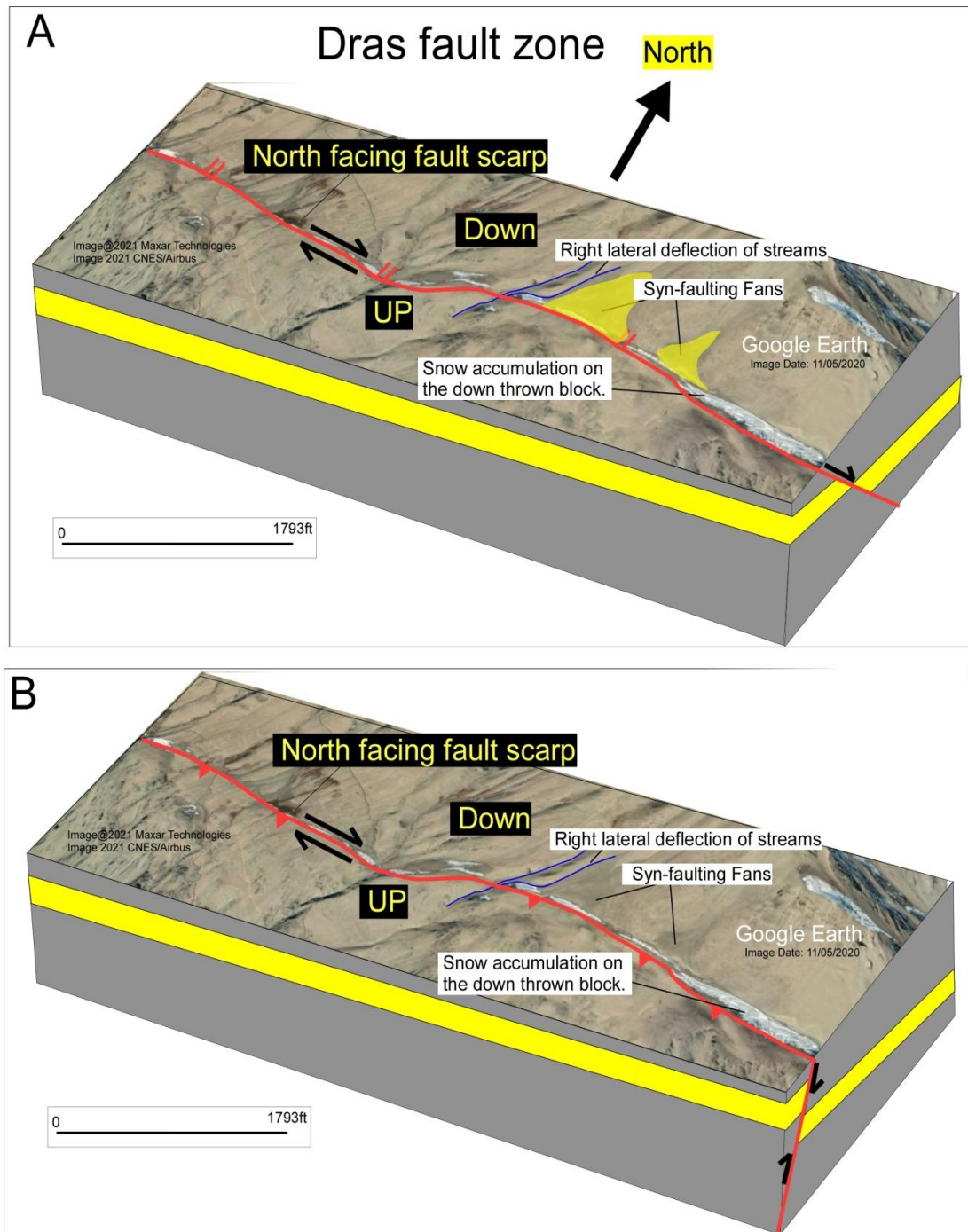
Figure 6. The trace of the Dras fault zone is mapped on the 3D Google satellite image. The fault is observed to have cut across the Holocene sediments, which suggest active faulting. The streams are offset, and the snow has accumulated on the northern facing portion of the fault scarp that has given a unique appearance to the fault. Several fans have formed after faulting, which suggests the age of faulting could be the age of sediment accumulation. The upthrown (A) and the downthrown blocks are used to interpret the possible component of dip-slip on the fault, which suggests that the fault is either an oblique normal fault (A) or oblique backthrust (B).
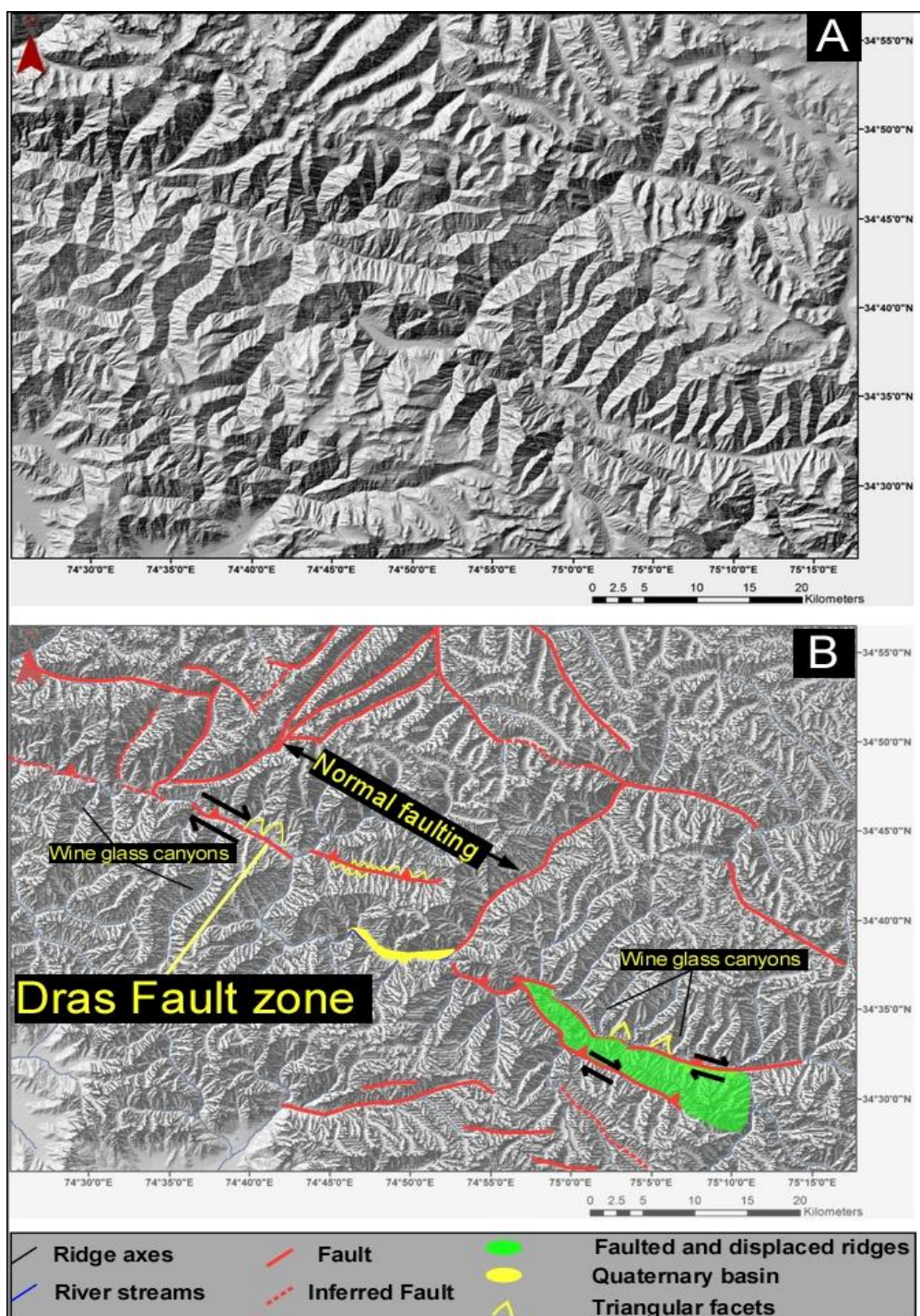
Figure 7. The uninterpreted 30 m shuttle radar topography is shown above (A), which is interpreted below (B). The tectonic geomorphology reveals that the western portion of the Dras fault zone is mostly represented by rugged topography where the direct evidence of active faulting is not convincing. However, the linearity of major streams suggests faulting. It is also confirmed by the ridge axes that are discontinuous and suggest faulting. The triangular facets are well preserved along some portion of the fault, which also suggests active faulting. The ~NW-SE trending faults are consistent with the strike of the Dras fault zone, which are cut by ~NE-SW trending normal faults. The location is shown in Figure 2.
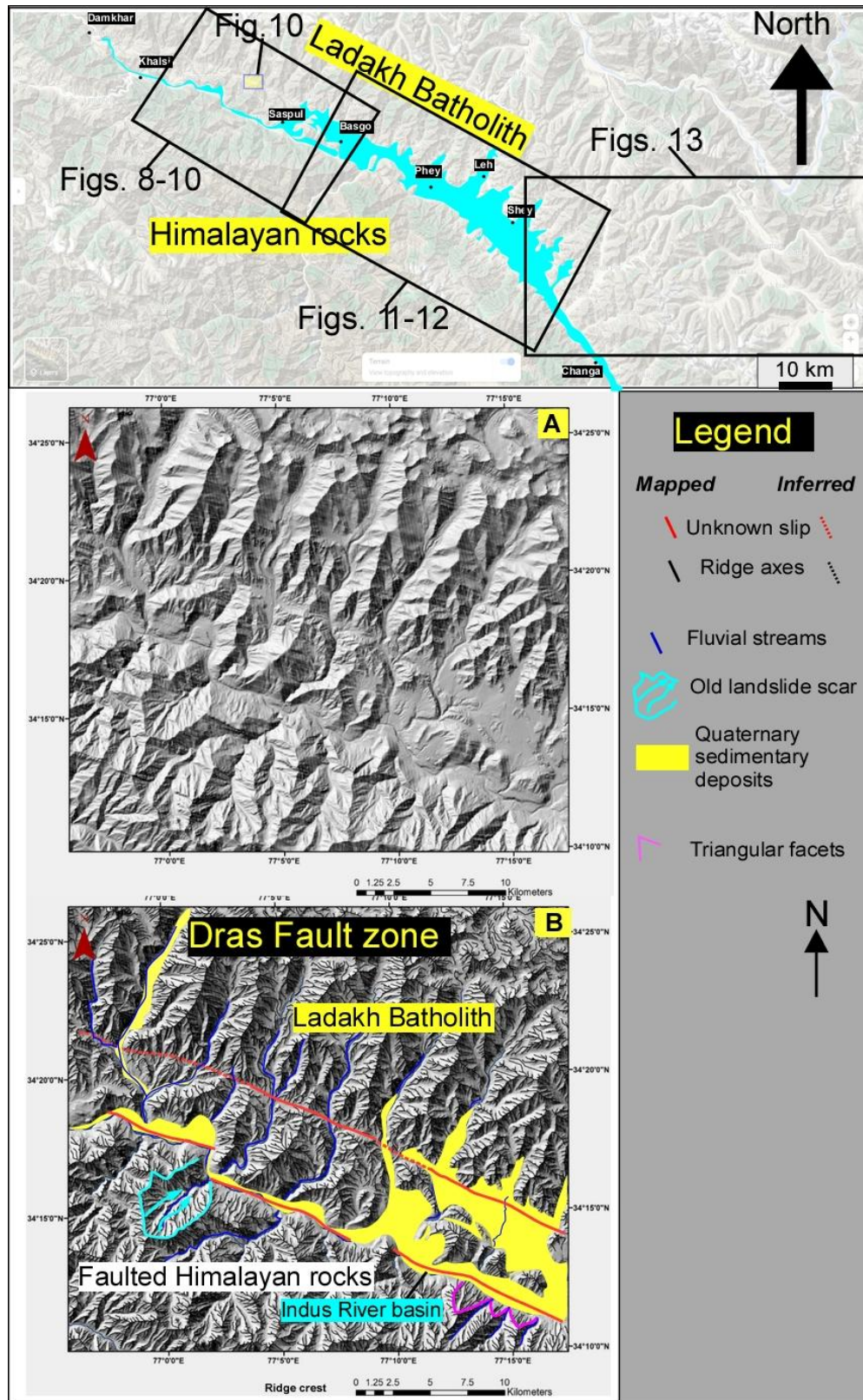
Figure 8. The uninterpreted 30m shuttle radar topography is shown above (A) and it is interpreted below (B). A clear zone of active faulting is mapped in the northwestern portion of the Leh Basin where the Holocene deposits are faulted. The location is in the upper panel of the figure.
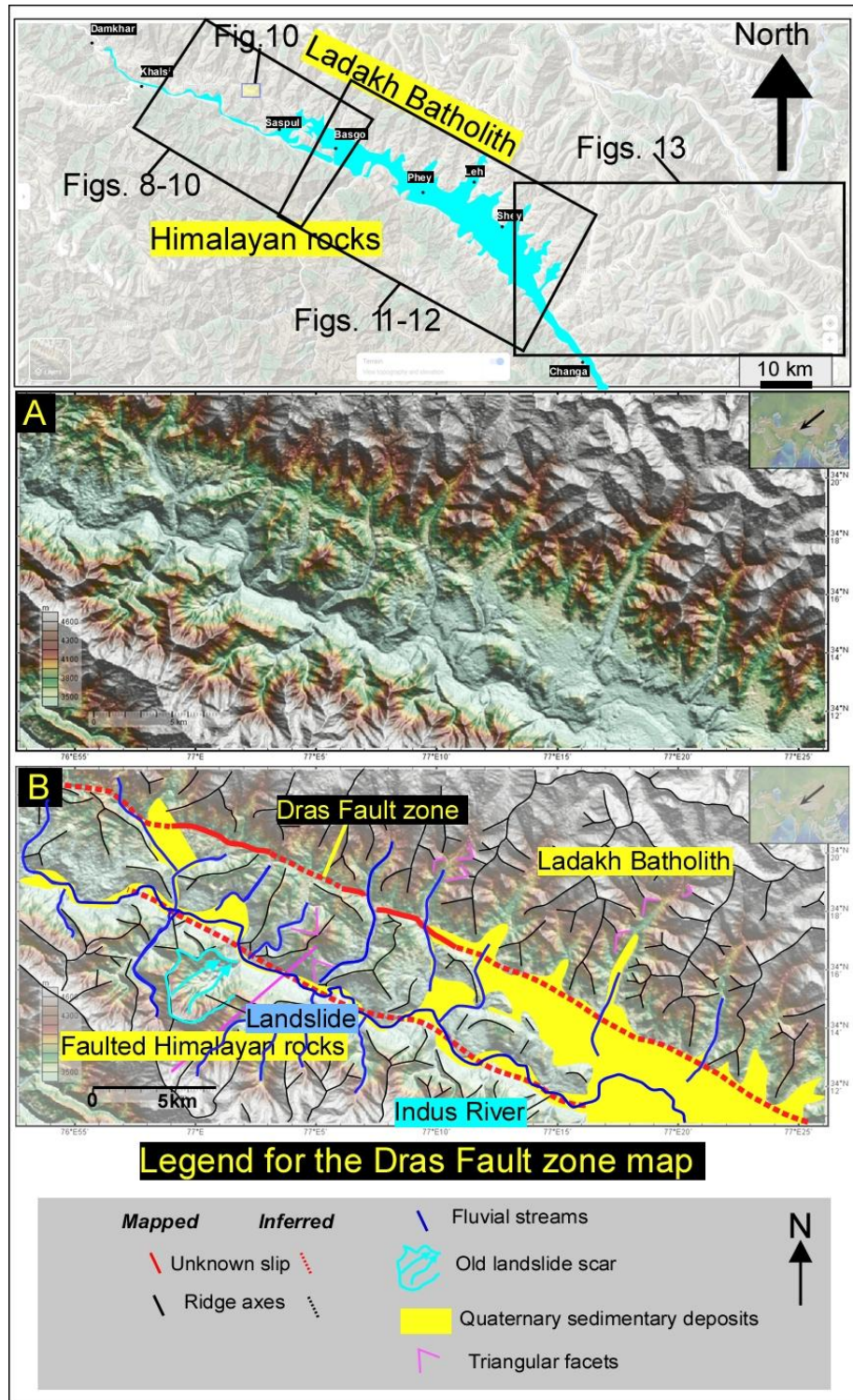
Figure 9. (A) The uninterpreted satellite image shows the western portion of the Leh basin, which is interpreted below (B). The fault is active, which is suggested by the faulted and displaced Holocene sediments. A paleo-landslide scar is mapped that could have dammed the Indus River and caused flooding and lake formation in the eastern portion of the basin where lake deposits are commonly found (see Figure 12). The location is in the upper panel of the figure.
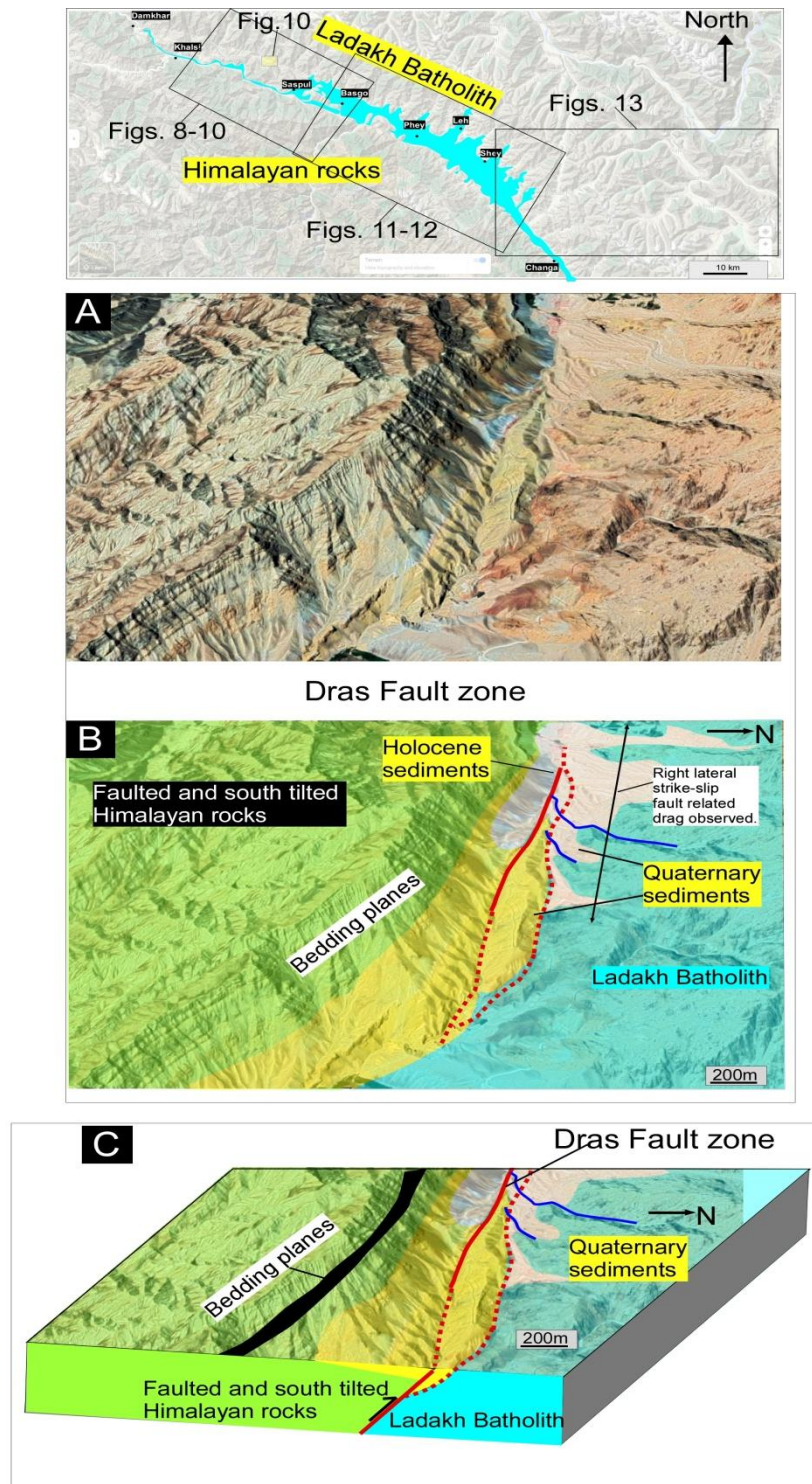
Figure 10. The uninterpreted image is shown above (A), and it is interpreted below (B). The active faulting has displaced Holocene aged river and lake deposits (shown in yellow). The northern portion of the image suggests the dextral strike-slip drag on rivers. The bedding layers of the Himalayan rocks are dipping towards the south, which suggests the south-dipping reverse fault (C). The location is in the upper panel of the figure.
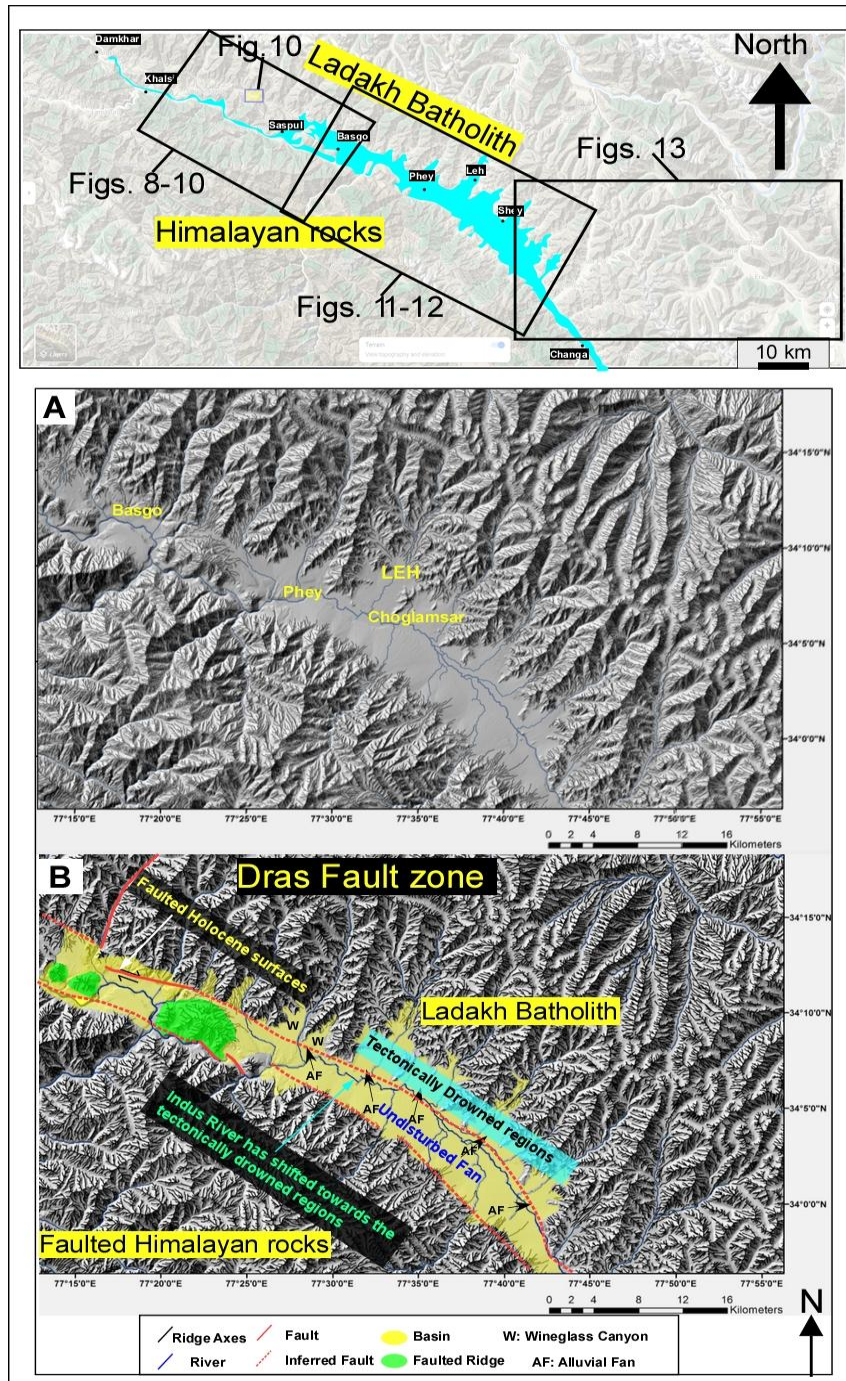
Figure 11. The uninterpreted shuttle radar topography shows the position of narrow oval-shaped Leh basin (A) that is surrounded by the rugged topography. The details suggest that the Quaternary sediments are faulted (B), which indicates active faulting. The fault scarp was mapped in the western portions where dextral strike-slip displacement was suggested by the deformed Holocene surfaces. The Indus River has been pushed towards the northeast by the prograding fan, which was marked as undisturbed by faulting on the map view. The northeastern portions of the Leh basin are tectonically drowned as suggested by the tectonic topography, which could cause the shifting of the Indus River towards the subsided regions. We have interpreted the basin as the pull-apart basin of the Dras fault zone as related to the curling of the basin. The location is in the upper panel of the figure.
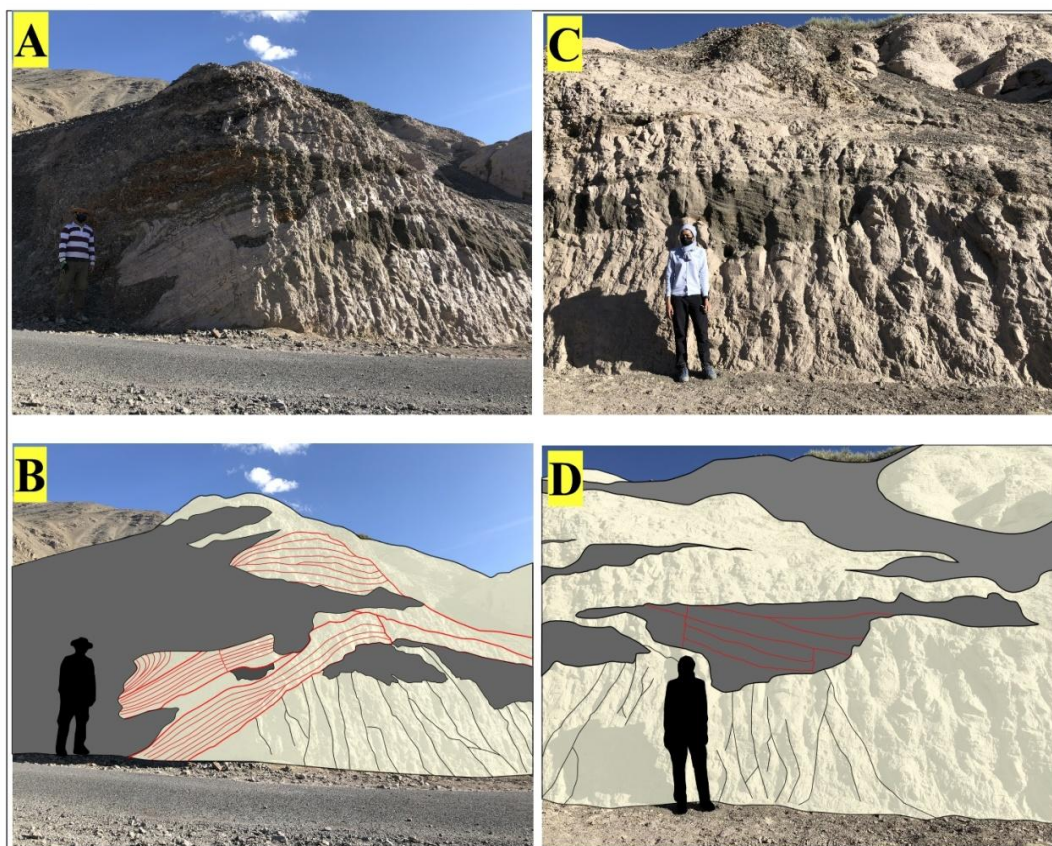
Figure 12. The disruption of the lacustrine facies related sediments with the coarse-grained alluvial fan-related sediments are interpreted as lake breaching event(s). The sediment disruption seems non-tectonic and could be related to landslides or any other non-tectonic causes. The photo was taken looking southwest at 34°7'14.81 N/77°25'16.908" E. Another example of lake disruption related sediment deformation (C and D), which could be non-tectonic as such features are local in extent and not reported throughout the extent of the Dras Fault zone. The photo was taken looking southwest at 34°7'14.52 N/77°25'16.77 E.

4.4. Fieldwork in the Leh region

Several field sites that we visited show clear evidence for soft-sediment deformation (e.g. Figure 12) but convincing evidence for active faulting is not observed. Therefore, we interpret the lack of evidence for active faulting to the thick sediment accumulation that could have blanketed the rupture zones that we could easily mark in the western portions and in the Dras Valley. Figure 12 shows glaciofluvial altered complex moraine deposits interlocked with glacial and lacustrine deposits. The interbedded lacustrine layers are truncated, and coastal onlap features are highlighted which suggests that the glacial conglomerate deposits were formed later. The active disruption of lacustrine deposit layers by the coarse-grained conglomerate facies is possibly an outcome of scouring and gravity sliding [35] and not active tectonics. The non-tectonic disruption and soft-sediment deformation could occur in several ways, which would usually initiate lateral compression, ductile and local extent of brittle deformation. A similar scenario was observed at other locations (Figure 12C), where we have mapped diamictite of sheet layer deposits, which specify extensive glacial

melting in the area. The stratified dark coloured lake deposits caught in the middle of Quaternary sand and silt deposits suggest non-tectonic disruption, which could occur by a landslide, or a major debris fall. The outcrop contains piles of sediments, such as fluvial and lacustrine where the lacustrine deposits are highlighted by stratified sedimentary beds inter-bedded with silty-sand layers. The debris flow could be organic-rich deposits as the terraces are made of dark organic-rich clayey silt.

The tectonic topography related to the Ladakh Batholith Fault zone is highlighted (Figure 13). The fault zone is well developed and cuts through the batholith (Figure 13B). We think it could be a normal fault as similar faults are mapped in the east that pierces through the batholith.

4.5. Seismological and earthquake centroid moment tensor (CMT) data

The earthquake events plotted on the shuttle radar topography shows patches of concentrated regions that are largely restricted in the northwest and southeast of the Kashmir basin (Figure 3A). The section across the fault shows shallow seismicity (Figure 3B) in the Dras fault zone area. However, the study area is mostly devoid of earthquakes and only a small number of events are observed. These are mostly aligned with the Dras fault zone and could be associated with it. However, the events are smaller and therefore, the CMT solutions are not available to make such interpretations (Figure 2B) more acceptable. The detailed analysis of representative CMT events shows that the region is actively undergoing thrust, normal and strike-slip faulting (Figure 2). The normal faults are ~NE-SW trending, which is ~orthogonal to the strike of the reverse and strike-slip faults and suggests ~NW-SE extension is actively occurring in the India-Eurasia collision zone where ~NE-SW tectonic scale compression is active and reflected by the occurrence of reverse, thrust, and strike-slip faults. The Dras fault fits the regional compression and would be expected to kinematically resemble an oblique reverse fault system.
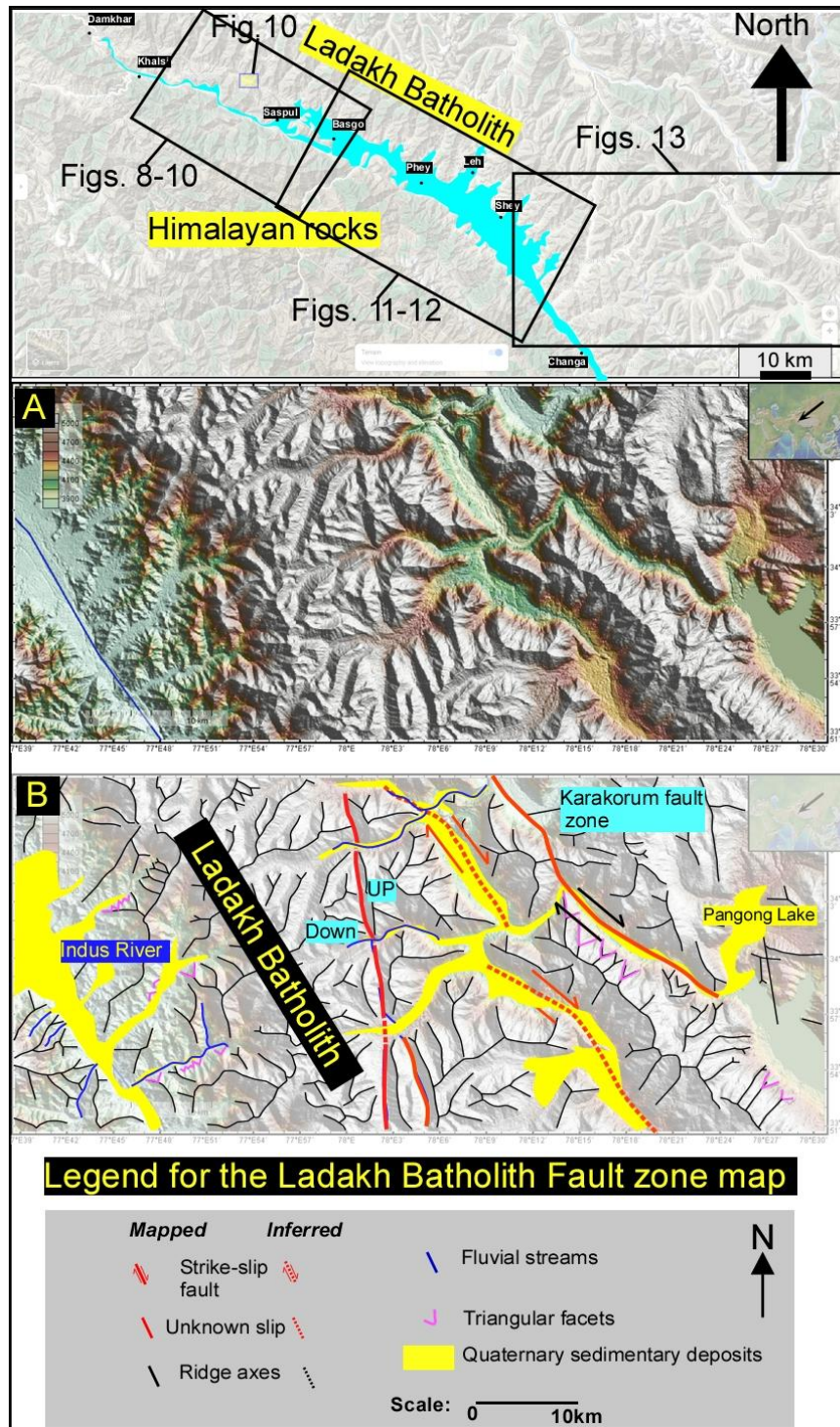
Figure 13. The tectonic topography related to the Ladakh Batholith Fault zone is highlighted (A). The fault zone is well developed and cuts through the batholith (B). We think it could be a normal fault as such faults are mapped in the east that pierces through the batholith. The location is shown in Figure 1. The location is in the upper panel of the figure.

5. Discussion

5.1. Dras fault: active faulting in the Himalayan suture zone

The well-preserved fault scarps, displaced rivers, ridges, and Holocene sediments provide excellent evidence for active faulting in the Indus Suture Zone (ISZ), which is the first such convincing confirmation to demonstrate active faulting in suture zone regions in NW Himalaya. The total length of the fault zone is exposed as 2 major strands that are separated by a ridge, which fits a restraining bend geometry for the Dras fault (Figure 14). The eastern portion of the fault can be observed to have ruptured the Holocene sediments in the Leh basin, and further west it possibly merges with the Karakoram fault system (Figure 14). The western portion of the Dras fault is not clearly mappable in the rugged topography with only a few small, isolated basins (Figure 7). The Kishanganga River/Neelum River follows the trace of the fault, and then the fault possibly merged with the purely reverse fault system in the far west (Figure 14). These structural relationships suggest that the Dras fault is an oblique fault that could be a reverse fault with a dextral strike-slip component. The Leh basin is a small linear basin that runs parallel to the fault, and it fits a pull-apart setting associated with a major fault with a component of dextral strike-slip motion. The small dimension of the basin supports our interpretation that the Leh basin has been created by the dextral strike-slip motion on the Dras fault system (Figure 11). The only confusion about the kinematics of the fault is whether it is reverse or normal. The most obvious fault trace is observed in the Dras region (Figures 4 to 6), and there the fault has ruptured the Holocene surfaces and displaced river terraces and fans. The hanging wall block is differentiated based on the up and down movement of the faulted blocks, which we have interpreted either as an oblique normal fault (Figure 6A) or an oblique reverse fault (Figure 6B). These two interpretations are possible because the kinematic indicators are not available as the field location is a politically sensitive area and therefore, fieldwork was not possible. The reverse slip means that the fault could be a major active oblique backthrust, and it is exactly located where the Indus Suture Zone (ISZ) has been mapped [36,37]. Therefore, it indicates that the suture zone is active, and the Dras fault zone is part of the fault system in the suture zone, and the backthrust geometry resembles the previously mapped Zanskar backthrust fault that has Zanskar Supergroup over the Lamayuru complex [37]. The suture zone is bounded on the south by the Zanskar Shear Zone (ZSZ). The Zanskar backthrust and the ZSZ perhaps intersect at the Dras region, and therefore, it makes it difficult to correlate the Dras fault with the previously mapped faults [37]. Nonetheless, the Dras fault is active and that is the major concern for the potential earthquake hazards associated with the fault.

Our fieldwork in parts of the Leh region suggests that the active faults are mostly probably hidden below the sediments. The soft-sediment deformation that we have observed is related to gravity deformation (Figure 12), and we have not observed convincing evidence in the field that could be related to active tectonics as has been suggested previously. Gravity tectonics seems to have created the soft-sediment deformation and resembles the features mapped in the Kashmir Basin [38].
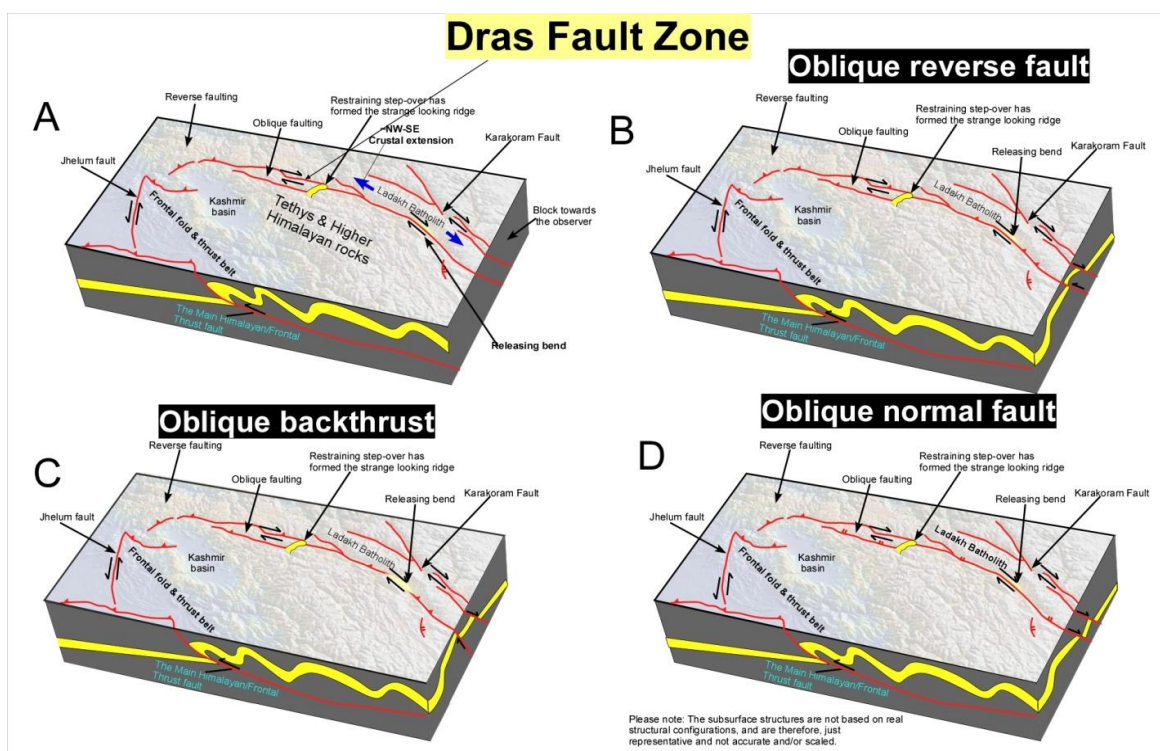
Figure 14. The 3D illustration shows the 30 m shuttle radar topography as the base map and the mapped active faults are traced on it (A). The subsurface extension of the faults and stratigraphy is not to scale. The Dras fault zone is interpreted based on our tectonic geomorphological observations and shown in the subsequent figures (B, C and D). The fault could be an oblique reverse fault, which requires that the upthrown block should be towards the north, which is not backed by the tectonic geomorphology as the upthrown block is located towards the south. Therefore, the fault is further interpreted either as an oblique backthrust (C), or an oblique normal fault (D). The fieldwork at the Dras region is required to map the actual kinematic details on faulting.

5.2. Dras fault zone and geodetic data

The tectonic geomorphology of the Dras fault zone clearly suggests active faulting in the Neogene to Quaternary deposits, which is mainly observable in the Dras and northwestern portion of the Leh basin. The active faulting suggests that the ongoing crustal deformation related to the plate convergence between India and Eurasia is not just limited to the frontal portions of the orogen but spread across the orogen with recent evidence of faulting in the Indus Suture Zone. The faulting at the Dras region shows strike-slip displacement along with some variation in topography that indicates dip-slip (Figure 6). The upthrown and downthrown blocks suggest that the fault is oblique, and possibly has a component of dip-slip motion, which could be related to reverse or normal slip. Since the fieldwork was not possible in the region, therefore, we have used the previously published geodetic data to understand the kinematics of the Dras fault zone. The fault fits the geodetic dataset where a strike-slip or oblique fault was expected in the NW Himalayan regions, but the geological and geomorphological evidence was lacking [39,40]. The well-known dextral strike-slip fault system, the Karakoram fault (KF), could be a good choice to accommodate the expected geodetically derived shearing component, which is $\sim 5 \pm 1$ mm/yr [40]. However, our data suggest that the Dras fault is the

best choice to accommodate the shear component in the Kashmir Himalayas, and it supports the interpretation of [41] who argues that the long-term slip rate on the KF system would not be adequate to interpret the obliquity of the GPS vectors. Therefore, we suggest that the Dras fault is the main structure that accommodates the shear component, and it is actively doing that.

The total length of the fault zone is >540 km, which is broadly divided into two major strands that are separated by curling of a ridge, and that we have interpreted as the restraining bend of the Dras fault zone. The eastern fault strand runs through the Leh basin, which we have interpreted as the pull-apart basin that is related to the releasing bend of the Dras fault (Figure 14A). The small dimensions of the basin suggest little strike-slip displacement and more dip-slip components. Therefore, the Dras fault could be an oblique backthrust that roots from the Karakoram fault zone (Figure 14). A series of ~NE-SW trending normal faults are also mapped on the ~NW and ~SE portions of the Dras fault zone, and it suggests that the region is undergoing simultaneous compression and extension. Previous work has mapped several ~NNE-SSW trending active normal faults in the Kashmir Himalaya [42], and these lie mostly orthogonal to the regional plate tectonic convergence. The absence of large-scale strike-slip displacement at the Dras fault zone could be attributed to normal faults, which are suitable structures to compensate for the crustal extension.

5.3. Seismological and Earthquake Centroid Moment Tensor (CMT) data

The shallow focus earthquake events (Figure 2) are distributed within the study area and suggest shallow crustal faulting that has originated mostly at <40 km. These earthquakes are restricted between the Karakorum fault and the Jhelum fault zones and suggest a major fault that would fit the structural configuration of the Dras fault zone (Figure 14). Therefore, it is suggested that the Dras fault zone is a ~NW-SE trending fault and connects to the Karakorum fault in the east and forms a loop in the east above the Kashmir basin where it emerges as an oblique reverse fault system (Figure 14).

The CMT events show that active deformation in NW Himalaya is mainly compensated by reverse and thrust faulting in the frontal portions and normal and strike-slip faulting in the interior regions (Figure 2B). These deformation patterns are observed in the east of the Jhelum fault, and interestingly, the ~NE-SW trending normal faulting events are located on the hanging-wall portion of the Dras fault system, and we interpret it as the direct consequence of oblique faulting, which is related to the India-Eurasia collision that has created simultaneous crustal extension perpendicular to the direction of the ~NNE-SSW direction tectonic compression (Figure 1). The ~NNW-SSE trending strike-slip fault events near the Karakoram fault zone are related to the fault and suggest dextral strike-slip movement. The Dras fault zone is possibly connected with the Karakoram fault in the east, while in the west, it is observed to be part of the ~NNE-SSW trending reverse faults, which indicates that the fault is curled in the west and shows a strong reverse slip (Figure 14).

6. Conclusions

The active Dras fault system in the Northwest portions of Himalaya is a striking example of oblique thrusting in the hinterland regions and shows that the ongoing plate convergence between India and Eurasia is not just limited to the frontal portions but spreads well into the core of the orogen. The fault merges with the reverse fault system in the west and the Karakoram fault in the east, which reflects its role in the tectonic convergence budget of the Himalayas. The earthquake

centroid moment tensor and the tectonic geomorphological data suggest that the region is actively undergoing compression, and extension, as is witnessed in the adjacent region of Tibet. Therefore, strike-slip, reverse, and normal faults are common in the region. The Dras fault seems to fit an oblique backthrust geometry, but an oblique normal fault will form a similar geometry. Fieldwork in the Dras regions will illuminate several uncertainties in terms of the kinematics of the fault and to know the chronological profile of the earthquakes on the fault system [e.g., 43,44]. The fault is in a politically sensitive area between India, Pakistan, and China, and therefore, the fieldwork would need collaboration between these countries, and in particular India where most of the field locations are located. Further, we have used the freely available 30 m shutter radar topography, which cannot offer details of the fault zone that are possible by using better resolution imagery. Therefore, it is recommended that higher resolution satellite images could reveal details that can add more revilement to the mapping shown here.

Data resources

The topographic images, earthquake centroid moment tensor events and earthquakes are obtained from the open-source web portal, www.geomapapp.com, last accessed January 2021. The field data are collected in Leh, India, in 2018, and details are in the Methodology section of the manuscript.

Acknowledgements

Conflict of interest

The authors declare no conflict of interest.

References

1. Shah AA, Addly AABM, Samat MIBA (2018) Geomorphic Mapping Reveals NW-SE Extension in NW Himalaya. *Arab J Geosci* 385–389.
2. Baker DM, Robert J, Robert S, et al. (1988) Development of the Himalayan frontal thrust zone: Salt Range, Pakistan. *Geology* 16: 3–7.
3. Yeats RS, Nakata T, Farah A, et al. (1992) The Himalayan frontal fault system. *Ann Tecton* 6: 85–98.
4. Wesnousky SG, Kumar S, Mohindra R, et al. (1999) Uplift and convergence along the Himalayan Frontal Thrust of India. *Tectonics* 18: 967–976.
5. Malik JN, Sahoo AK, Shah AA (2010) Paleoseismic evidence from trench investigation along Hajipur fault, Himalayan Frontal Thrust, NW Himalaya: implications of the faulting pattern on landscape evolution and seismic hazard. *J Struct Geol* 32: 350–361.
6. Wesnousky SG, Kumahara Y, Chamlagain D, et al. (2017) Geological observations on large earthquakes along the Himalayan frontal fault near Kathmandu, Nepal. *Earth Planet Sci Lett* 457: 366–375.

7. Coudurier-Curveur A, Tapponnier P, Okal E, et al. (2020) A composite rupture model for the great 1950 Assam earthquake across the cusp of the East Himalayan Syntaxis. *Earth Planet Sci Lett* 531: 115928.

8. Cloos M (1993) Lithospheric buoyancy and collisional orogenesis: Subduction of oceanic plateaus, continental margins, island arcs, spreading ridges, and seamounts. *Geol Soc Am Bull* 105: 715–737.

9. Tapponnier P, Molnar P (1977) Active faulting and tectonics in China. *J Geophys Res* 82: 2905–2930.

10. Keller EA (1986) Investigation of active tectonics: use of surficial earth processes. *Tectonics* 1: 136–147.

11. Malik JN, Nakata T (2003) Active faults and related late Quaternary deformation along the northwestern Himalayan frontal zone, India. *Ann Geophys* 46: 917–936.

12. Shah AA (2013) Earthquake geology of Kashmir Basin and its implications for future large earthquakes. *Int J Earth Sci* 102: 1957–1966.

13. Shah AA, Sahari S, Navakanesh B, et al. (2021) Tectonic geomorphology of the Jhelum fault zone and its contiguous regions in western Himalaya. *Bull Geol Soc Mal* 73.

14. Zhao LS, Xie J (1993) Lateral variations in compressional velocities beneath the Tibetan Plateau from Pn travel time tomography. *Geophys J Int* 115: 1070–1084.

15. Yin A (2000) Mode of Cenozoic east-west extension in Tibet suggesting a common origin of rifts in Asia during the Indo-Asian collision. *J Geophys Res* 105: 21745–21759.

16. Stevens VL, Avouac JP (2015) Interseismic coupling on the main Himalayan thrust. *Geophys Res Lett* 42: 5828–5837.

17. Shah AA (2015) Kashmir basin fault and its tectonic significance in NW Himalaya, Jammu and Kashmir, India. *Int J Earth Sci* 104: 1901–1906.

18. Sahoo S, Malik JN (2017) Active fault topography along Kangra valley fault in the epicentral zone of 1905 Mw7. 8 earthquake NW Himalaya, India. *Quat Int* 462: 90–108.

19. Burg JP, Bouilhol P (2018) Timeline of the South-Tibet—Himalayan belt: the geochronological record of subduction, collision, and underthrusting from zircon and monazite U-Pb ages. *Can J Earth Sci* 56: 1318–1332

20. Shah AA, Abd MN, Aliudin NAB, et al. (2020) Formation, Rotation, and Present-Day Configuration of Kashmir and Peshawar Basins in NW Himalaya. *Front Earth Sci* 8: 569771.

21. Yin A, Harrison TM (2000) Geologic Evolution of the Himalayan-Tibetan Orogen. *Annu Rev Earth Planet Sci* 28: 211–280.

22. Murphy MA, Yin A (2003) Structural evolution and sequence of thrusting in the Tethyan fold-thrust belt and Indus-Yalu suture zone, southwest Tibet. *GSA Bull* 115: 21–34.

23. Sinclair HD, Jaffey N (2001) Sedimentology of the Indus group, Ladakh, northern India: Implications for the timing of initiation of the palaeo-Indus River. *J Geol Soc* 158: 151–162

24. Garzanti E, Haver TV (1988) The Indus clastics: Fore-arc basin sedimentation in the Ladakh Himalaya (India). *Sediment Geol* 59: 237–249.

25. Searle MP, Pickering KT, Cooper DJW (1990) Restoration and evolution of the intermontane Indus molasse basin, Ladakh Himalaya, India. *Tectonophysics* 174: 301–314.

26. Searle MP (1986) Structural evolution and sequence of thrusting in the High Himalayan, Tibetan—Tethys and Indus suture zones of Zanskar and Ladakh, Western Himalaya. *J Struct Geol* 8: 923–936.

27. Qayyum M, Lawrence RD, Niem AR (1997) Discovery of the palaeo-Indus delta-fan complex. *J Geol Soc* 154: 753–756.

28. Nakata T (1989) Active faults of the Himalayas of India and Nepal. *Spec Pap Geol Soc Am* 232: 243–264.

29. Sahoo S, Malik JN (2017) Active fault topography along Kangra valley fault in the epicentral zone of 1905 Mw7. 8 earthquake NW Himalaya, India. *Quat Int* 462: 90–108.

30. Shah AA, Syaakiirroh Sahari, Navakanesh B, et al. (2022) Tectonic geomorphology of the Jhelum fault zone and its contiguous regions in western Himalaya. *Bull Geol Soc Malay* 73.

31. Shah AA, Navakanesh B (2020) Active tectonics and active faults: Why these terms still lack consensus on definitions. *Bull Geol Soc Malay* 70: 125–132.

32. DiPietro JA, Pogue KR (2004) Tectonostratigraphic subdivisions of the Himalaya: A view from the west. *Tectonics* 23.

33. Jouanne F, Munawar N, Mugnier JL, et al. (2020) Seismic coupling quantified on inferred décollements beneath the western syntaxis of the Himalaya. *Tectonics* 39.

34. Shah AA, Rajasekharan A, Batmanathan N, et al. (2021) Dras Fault: a major active fault in Kashmir Himalaya. *Bull N Z Soc Earthq Eng* 30.

35. Sangode SJ, Phadtare NR, Meshram DC, et al. (2011) A record of lake outburst in the Indus valley of Ladakh Himalaya, India. *Curr Sci* 100: 1712–1718.

36. Gansser A (1980) The significance of the Himalayan suture zone. *Tectonophysics* 62: 37–52.

37. Searle MP (1983) Stratigraphy, structure and evolution of the Tibetan-Tethys zone in Zanskar and the Indus suture zone in the Ladakh Himalaya. *Earth Environ Sci Trans R Soc Edinb* 73: 205–219.

38. Ahmad SA, Sahari S, Qadir A, et al. (2020) A critical review of field relationships and gravitational origin of active normal faults in the Kashmir basin, NW Himalaya. *J Asian Earth Sci X* 100042.

39. Schiffman C, Bali BS, Szeliga W, et al. (2013) Seismic slip deficit in the Kashmir Himalaya from GPS observations. *Geophys Res Lett* 40: 5642–5645.

40. Kundu B, Yadav RK, Bali BS, et al. (2014) Oblique convergence and slip partitioning in the NW Himalaya: Implications from GPS measurements. *Tectonics* 33: 2013–2024.

41. Bilham R (2019) Himalayan earthquakes: a review of historical seismicity and early 21st century slip potential. *Geol Soc Spec Publ* 483: 423–482.

42. Omar Pengiran DNA, Shah AA, Abd MN (2020) Active transtensional structures mapped in the west of Karakoram fault (KF), Kashmir Himalayas. 5th International Young Earth Scientists (YES) Congress "Rocking Earth's Future".

43. Koukouvelas IK, Zygouri V, Papadopoulos GA, et al. (2017) Holocene record of slip-predictable earthquakes on the Kenchreai Fault, Gulf of Corinth, Greece. *J Struct Geol* 94: 258–274.

44. Koukouvelas IK, Zygouri V, Nikolakopoulos K, et al. (2018) Treatise on the tectonic geomorphology of active faults: The significance of using a universal digital elevation model. *J Struct Geol* 116: 241–252.